Clear-air Turbulence Effects Modeling on Terrestrial and Satellite Free-Space Optical Channels

F.S. Marzano[1], D. Carrozzo[1], S. Mori[1], F. Moll[2]

[1] Dept. of Information Engineering, Electronics and Telecommunications (DIET)
Sapienza University of Rome, Rome, Italy
marzano@diet.uniroma1.it, mori@diet.uniroma1.it, dnt.carrozzo@gmail.com

[2] Institute of Communications and Navigation, German Aerospace Center (DLR)
Oberpfaffenhofen, D-82234 Wessling, Germany
Florian.Moll@dlr.de

***Abstract*—Wireless communications using free space optics (FSO) are sensitive to atmospheric conditions. Clear-air turbulence can introduce severe impairments reducing FSO channel availability. Radiosounding profiles, available near Rome (Italy) and Munich (Germany), are used to estimate the power scintillation index through a new physical refractive index structure constant model and to estimate scintillation fade statistics for near-infrared FSO. Preliminary qualitative validation is performed using FSO campaign near Munich for both terrestrial and slant links.**

Keywords—free space optics, atmospheric turbulence, optical modelling, meteorological data, scintillation fade.

I. INTRODUCTION

Free Space Optics (FSO) represent a promising technology and, at the same time, a complementary choice to radio frequency (RF) peer-to-peer links and wide area networks (WANs) [1]-[3]. FSO can allow line-of-sight links of several kilometers in optimal conditions, but an acceptable quality of service (QoS) can be guaranteed only for shorter ranges. In fact, atmospheric effects are perhaps the biggest challenge in FSO because they can limit operating avaliability [4], [5].

FSO links are very sensitive to the presence of atmospheric droplets within the beam such as fog and hydrometeors [4], [6]-[10]. Tropospheric turbulence, due to small temperature variations of atmopsheric masses, can be responsible of beam power losses due to the beam spot spreading and of space-time fluctuations of the laser beam intensity, better known as scintillation [6].

In this paper we will briefly summarize a physical model of refractive index structure constant and scintillation (Sect. II). We will then apply it to radiosounding profiles (Sect. III) and compare with FSO channel data (sect. IV), in order to perform a preliminary validation using available measurements. Conclusions will be drawn in Sect. V.

II. FSO SCINTILLATION MODEL

Atmospheric turbulence is often represented as a cascade of air eddies with different temperature, humidity and density thus inducing a random space-time varibility of the refractive index [3]. This effect causes electro-magnetic scintillation: the fluctuation of amplitude and phase of the optical beam transmitted through atmospheric turbulence [5].

The structure constant of the atmospheric refractive index for optical applications can be expressed as [6]:

$$C_n^2(z;T) = \left(\frac{80\ 10^{-6}p}{T^2}\right)^2 C_T^2(z) = a^2(K_H/K_M)L_0^{4/3}\left(\frac{\partial T}{\partial z}\right)^2 \quad (1)$$

where $a^2=2.8$ is an empirical constant, K_H/K_M = 1.35 (the ratio is the exchange coefficients for heat and momentum) [7], C_T^2 the temperature structure constant and L_0 is the spatial outer scale.

An update model of the refractive index structure constant has been recently presented taking into account the conservative passive additive property of potential temperature θ [8] and applied to FSO [14]. If T is absolute temperature (K) and p is pressure (hPa), then potential temperature θ is defined by [5]:

$$\theta = T\left(\frac{p_0}{p}\right)^{R/C_p} \quad (2)$$

where p_o is the reference pressure (at 1000 hPa), R is the air gas constant, c_p is the specific heat capacity (with R/c_p = 0.286).

The rigorous final expression of C_n^2 then becomes [8], [14]:

$$C_n^2(z;\theta) = \left(\frac{80x10^{-6}p}{T\theta}\right)^2 C_\theta^2(z) \quad (3)$$

where potential temperature structure constant is given by:

$$C_\theta^2(z) \cong a^2(K_H/K_M)L_0^{4/3}\left(\frac{\partial \theta}{\partial z}\right)^2 \quad (4)$$

In the weak-fluctuation scintillation theory the Rytov log-amplitude variance parameter is expressed by [6]:

$$\sigma_R^2 = 1.23k^{7/6}\int_0^L C_n^2(r)r^{5/6}dr \quad (5)$$

This work has been carried out within JLAP project between ISCOM-MISE (Rome, Italy) and DIET Sapienza University of Rome (Italy) and within the COST-IC1101 OPTICWISE framework.

Postprint. Original IEEE article: F.S. Marzano, D. Carrozzo, S. Mori, and F. Moll, "Clear-air Turbulence Effects Modeling on Terrestrial and Satellite Free-Space Optical Channels," in 2015 4th International Workshop on Optical Wireless Communications (IWOW), pp. 36-40, Sept. 2015 doi: 10.1109/IWOW.2015.7342261

where $k=2\pi/\lambda$ the wavenumber, r is the range and L the length path. For terrestrial optical link (TOL), if $C_n^2(r) \equiv C_n^2(0)$ with $C_n^2(0)$ the near-surface refractive index structure constant, then for horizontal paths it holds [14]:

$$\sigma_R^{2\,TOL} = 1.23k^{7/6}L^{11/6}C_n^2(0) \qquad (6)$$

For satellite optical link (SOL) [6], if a vertically stratified atmosphere and slant paths is supposed, we can write:

$$\sigma_R^{2\,SOL} = 2.25k^{7/6}sec^{11/6}(\alpha)\int_{z_0}^{H} C_n^2(z)(H-z)^{5/6}dz \qquad (7)$$

where α is the link zenith angle, H the maximum height of the link path (H = 12000 m in this work) and z_0 the surface level.

In order to take into account the aperture-averaging factor, f_{AA} quantifies the reduction of scintillation due to the lens aperture of diameter D_{RX} [9]:

$$\sigma_P^2 = f_{AA}(D_{RX})\sigma_I^2 \qquad (8)$$

where the variance σ_P^2 of received scintillation power, scaled by the square of the mean power $\langle P_{RX}\rangle$, is called the power scintillation-index and σ_I^2 is the intensity scintillation-index.

Under strong fluctuation and plane wave assumption, the power scintillation index in (8) can be then expressed by [6]:

$$\sigma_P^2(D_{RX},L) = exp\left[\frac{0.49\sigma_R^2}{\left(1+0.65d^2+1.11\sigma_R^{12/5}\right)^{7/6}} + \frac{0.51\sigma_R^2\left(1+0.69\sigma_R^{12/5}\right)^{-5/6}}{1+0.9d^2+0.62d^2\sigma_R^{12/5}}\right] - 1 \qquad (9)$$

where $d^2 = (kD_{RX}^2/4L)$ is the ratio of the aperture size over the Fresnel zone size.

Note that the computation of C_n^2 with (3) and (4), which affects the evaluation of (9), needs the knowledge of the outer scale L_0 which delimits the lower frequencies of the inertial subrange of the refractive-index fluctuation spectrum in a well-developed homogeneous isotropic turbulence. Values of L_0 can range from few meters up in the planetary boundary layer (up to 1 km) to tens of meters in free atmosphere [6]. An empirical formula which provides the behavior of the outer scale with the altitude is (in m) [11]:

$$L_0(z) = 5/\left[1+\left(\frac{z-7500}{2500}\right)^2\right] \qquad (10)$$

The previous formula suggests L_0=0.5 m at surface, L_0 =5 m at 7.5 km and L_0 =1.2 m at 12 km.

III. Meteorological Sounding Data and Turbulence

Meteorological data is obtained from radio sounding observations (RAOB) in order to estimate a C_n^2 profile using equation (1) or (3).

A. Radiosounding data

In this work we have collected data from the RAOB station at Muenchen-Oberschleissheim (Munich, Germany). The processed RAOB data set refers to all the year 2000, having at disposal in particular two RAOBs per day (at 00:00 and 12:00 UTC). Observations were archived up to 12 km height. The specific meteorological data, available from each RAOB at a given level, are atmospheric pressure, geopotential height, temperature T, dewpoint temperature, relative humidity plus wind velocity and orientation.

With respect to [14], all profile data have been interpolated at the same height levels in order to perform a matrix computation by assuming standard vertical gradient behavior using a linear interpolation procedure to avoid lack of data.

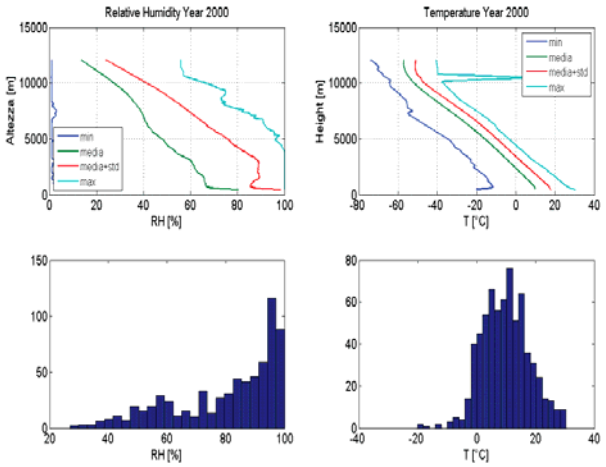

Fig. 1. Average annual profile of relative humidity and temperature, together with their near-surface value histogram using RAOB in 2000 at Muenchen-Oberschleissheim.

Fig. 1 shows the vertical profile of the annual mean temperature and relative humidity (plus deviation, minimum and maximum) together with its surface value histogram from all the year 2000 using at Muenchen-Oberschleissheim RAOB data set.

B. Turbulence structure constant

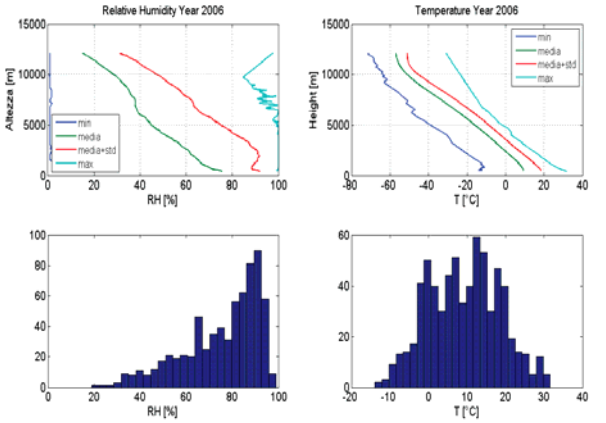

Fig. 2. Average annual profile of relative humidity and temperature, together with their near-surface value histogram using RAOB in 2006 at Muenchen-Oberschleissheim.

The C_n^2 profile statistics, using the T-dependent and θ-dependent models in (1) and (3), can be derived by exploiting data from Fig. 2. The 2 models are fairly comparable near the surface, but they significantly differ in the free atmosphere [14].

The outer scale L_0 has been set according to the empirical formula in (10).

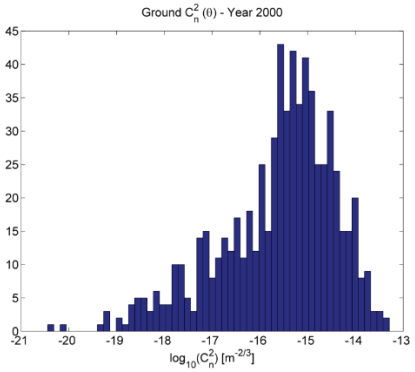

Fig. 3. Near-surface refractive index structure constant, derived from the application of formula (3) for Muenchen-Oberschleissheim RAOB dataset in 2000.

Fig. 3 shows the annual statistics of the near-surface C_n^2 derived from the same RAOB dataset. A range between 10^{-20} and 10^{-13} $m^{-2/3}$ are observed, as expected. A more detailed analysis (not depicted here) indicates, that higher values of the near-surface C_n^2 are typical during summer.

IV. RESULTS OF SCINTILLATION ANALYSIS

Coupling the available meteorological dataset with scintillation models of Sect. II, we can simulate the behaviour and statistics of the scintillation index for typical FSO links. Preliminary results will be discussed in the next paragraphs.

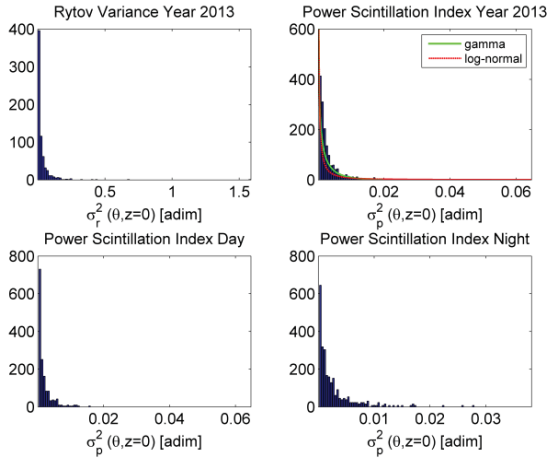

Fig. 4. Histogram of NIR power scintillation index and Rytov variance on terrestrial link using $C_n^2(\theta)$ model for a path length L=800 m, using RAOB dataset of Pratica di Mare (Rome, Italy) in 2013 and using a lens aperture of 10 cm. Log-normal and Gamma PDFs are also plotted for power scintillation index intercomparison.

A. *Simulated scintillation index for terrestrial link*

Using the scintillation model of Sect. II, we have evaluated the statistics of σ_I^2 for terrestrial link path (see (6) and (9)).

In this first analysis FSO system and path parameters are derived from the NIR (Near Infrared) link at 1550 nm in Rome (Italy) with L=800 m, a link about 20 km far from the nearest RAOB site in Pratica di Mare [10]. RAOB data of 2013 have been collected for this purpose. Statistical results in terms of Rytov variance σ_R^2 and power scintillation index σ_P^2 are shown in Fig. 4 and 5 for near surface RAOB data using 2 different lens apertures D_{RX}. Preliminary results seem to indicate NIR σ_P^2 less than 0.1 for the 2013 dataset. A numerical comparison with log-normal and Gamma analytical probability density functions (PDFs) in Fig. 4 indicates that the log-normal PDF could be an appropriate statistical best-fitting model.

As a further example for a preliminary validation, we have used measurements of an optical link setup at DLR (German Aerospace Center) during 2000 [12]. The transmitter of the experiment consists of a highly coherent 50mW Nd-YAG-laser emitting CW at 1064 nm. The transmitter is situated 400 m south of the receiver (15 m above ground on top of a tower). The 400-m path is horizontal. The scintillometer receiver features three apertures of different diameters (12, 22, and 48 mm) and a CCD-camera for beam-control [12].

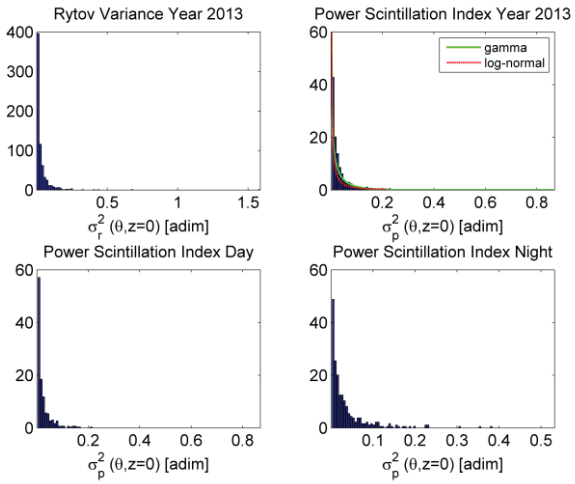

Fig. 5. Same as in Fig. 4, but for a lens aperture of 3.8 cm.

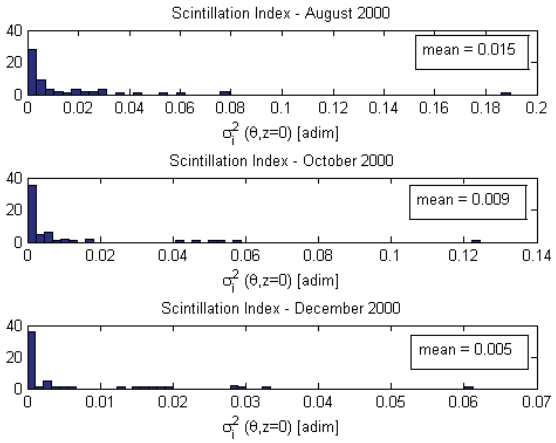

Fig. 6. Occurrences of simulated scintillation-index using RAOB data from the Muenchen-Oberschleissheim station during 2000, using λ = 1064 nm and L = 400 m in the year 2000 using for comparison with DLR measured data.

Preliminary results are shown in Fig. 6 where the histogram of the simulated scintillation index using RAOB data is shown for August, October and December 2000 and compared with DLR available measurements. Here, measured scintillation-index distributions over all measurements (irrespective of time of day) showed mean values in August of 0.037, in October of 0.028, and in December of 0.035 [12].

RAOB-based simulated mean values, labeled in each plot of Fig. 6, are quite comparable with those measured at DLR, considering that RAOB data are sampled twice a day whereas FSO measurements were gathered continuously every 10 minutes. Another reason for explaining the discrepancy between simulations and measurements is probably due to the adoption of a plane-wave model instead of a spherical-wave model.

B. Scintillation index for satellite link

Using the satellite link model of Sect. II (see (7) and (9)), we have also carried out the evaluation of NIR σ_I^2 for a slant link. In this case we have used published data from the optical LEO downlinks from the Japanese OICETS to the optical ground station, built by DLR, near Munich during the KIODO campaign in June 2006 [13]. The ground station received a 50-Mbit/s OOK signal at 847 nm on its 40-cm Cassegrain telescope and sent two spatially displaced beacon beams towards OICETS. The elevation angle above the horizon ranged between around 2° and 45° (see Fig. 7).

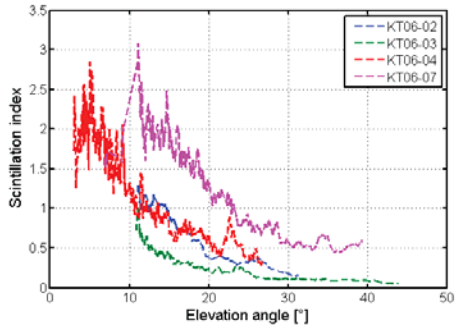

Fig. 7. Measurements carried out at DLR during the KIODO campaign in June 2006 near Munich for 4 days of June (Kiodo Trials 2006: KT06-XX) (from [13]). Measurement gaps are bridged with linear interpolation to better illustrate the saturation in KT06-07 and KT06-04.

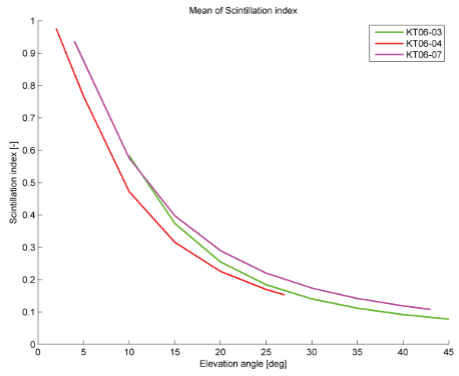

Fig. 8. Scintillation index as a function of the elevation angle for 3 days of June (KT06-XX) during the KIODO campaign in 2006. Wavelength is 847 nm for Earth-satellite slant paths.

Simulated scintillation index at 847 nm is shown in Fig. 8 as a function of the elevation angle for 3 days (14, 15, and 28 June 2006, labeled KT06-03, KT06-04, KT06-07) using a RAOB maximum height H=12000 m during day and night (above 12000 m. the turbulence structure constant contribution is negligible). If compared with clear-air measured curves of the KIODO campaign [13], preliminary analysis of Fig. 7 and Fig. 8 show that the agreement is quite good in KT06-03. However, scintillation index is underestimated in KT06-04/07 and the run of the curves do not fully agree for no saturation peak is visible in the simulations. Significant effects of post-thunderstorm environment are noted for KT06-07 day (June 28) [13] which shows the poorest agreement. The deviation of the simulated data from the measurements may have multiple origins: geographic separation of the measurement, inner scale effects which are not covered by the model in section II and still remaining errors in the C_n^2 modeling with the RAOB data. Especially the storm in KT06-07 may have caused severe turbulence differences in the two locations and thus strong deviation in scintillation index.

V. Conclusion

A model for simulating scintillation index for both horizontal and slant paths has been introduced. Its main feature is the exploitation of measured meteorological RAOB profile data, available twice a day all over the world.

Preliminary results about the validation of RAOB-based scintillation-index simulations have been shown by using published data of DLR experiments. These comparisons are encouraging, even though they should be performed on a more detailed and quantitative basis. The latter will be the goal of future work.

Acknowledgment

The authors deeply thank the staff of ISCOM (Ministry of Economic Development) for the cooperation within the ISOCM-DIET joint laboratory on antennas and propagation (JLAP). Dr. D. Giggenbach (VLC) is acknowledged for data references.

References

[1] COST Action IC1101, “Optical Wireless Communications - An Emerging Technology”, Memorandum of Understanding:, http://www.cost.esf.org/domains_actions/ict/Actions/IC1101, 2011.

[2] A.K. Majumdar and J.C. Ricklin *Free-Space Laser Communications, Principles and Advantages*. Springer Science LLC, 233 Spring Street, New York, NY 10013, U.S.A., 2008.

[3] A. Ishimaru, *Wave propagation and scattering in random media*, (IEEE Press, Piscataway (NJ), 453 pp., 1997.

[4] R. Nebuloni and C. Capsoni, “Effect of Hydrometeor Scattering on Optical Wave Propagation Through the Atmosphere”, Proc. of 5th European Conference on Antennas and Propagation (EuCAP), Rome (IT), 11-15 April 2011.

[5] V.I. Tatarski,, *Wave Propagation in a Turbulent Medium*. McGraw-Hill, 285 pp., 1961.

[6] L. Andrews and R. Phillips, *Laser Beam propagation trough Random Media*, Second ed,, SPIE Press, 782 pp., 2005.

[7] E. Masciadri, J. Vernin, and P. Bougeault, “3D mapping of optical turbulence using an atmospheric numerical model. I: A useful tool for the ground-based astronomy”, Astron. Astrophys. Suppl. Ser., vol. 137, pp. 185–202, 1999.

[8] T. Cherubini and S. Businger, “Another Look at the Refractive Index Structure Function”. J. Applied Meteorology and Climatology, vol. 52, p. 498-506, 2013.

[9] H. Henninger, and O. Wilfert, “An Introduction to Free-space Optical Communications”, Radioengineering, vol. 19, pp. 203-212, 2010

[10] F.S. Marzano, S. Mori, F. Frezza, P. Nocito, G.M. Tosi Beleffi, P. Lucantoni, M. Ferrara, and E. Restuccia, “Characterization of Hydrometeor Scattering Effects and Experimental Measurements Using Near-Infrared Free-Space Urban Links”, Proc. of 6th European Conf. on Antennas and Propagation (EuCAP) 2012, Prague, CZ, 26-30 March 2012.

[11] C.E. Coulman, J. Vernin, Y. Couquegniot, and J.L. Caccia, “Outer scale of turbulence appropriate to modeling the refractive-index structure profile”, Appl. Opt., vol. 27, pp. 155-160, 1988.

[12] D. Giggenbach, H. Henniger, F. David, “Long-Term Near-Ground Optical Scintillation Measurements”, Proc. SPIE, vol. 4976, 2003.

[13] N. Perlot, M. Knapek, D. Giggenbach, J. Horwath, M. Brechtelsbauer, Y. Takayama, and T. Jono, “Results of the Optical Downlink Experiment KIODO from OICETS Satellite to Optical Ground Station Oberpfaffenhofen (OGS-OP)”, Proc. SPIE, vol. 6457, 2007.

[14] D. Carrozzo, S. Mori, F.S. Marzano, “Modeling Scintillation Effects on Free Space Optical Links using Radiosounding Profile Data”, Proc. of the 2nd International Workshop on Optical Wireless (IWOW2014), Madeira (Portugal), 17-19 sept. 2014.